QCD analysis of first b cross section data at 1.96 TeV

Matteo Cacciari

Dipartimento di Fisica, Università di Parma, Italy, and
LPTHE, Université P. et M. Curie (Paris 6), France [*]
E-mail: `cacciari@lpthe.jussieu.fr`

Stefano Frixione

INFN, Sezione di Genova, Italy
E-mail: `Stefano.Frixione@cern.ch`

Michelangelo L. Mangano

CERN, Theoretical Physics Division, Geneva, Switzerland
E-mail: `Michelangelo.Mangano@cern.ch`

Paolo Nason

INFN, Sezione di Milano, Italy
E-mail: `Paolo.Nason@mib.infn.it`

Giovanni Ridolfi

INFN, Sezione di Genova, Italy
E-mail: `Giovanni.Ridolfi@ge.infn.it`

ABSTRACT: The first data on bottom quark production in $p\bar{p}$ collisions at 1.96 TeV have recently been obtained by the CDF collaboration. These data probe the region of $p_T \sim 0$, providing a new invaluable input on the issue of the compatibility between next-to-leading-order (NLO) QCD and data. We reconsider the evaluation of the b cross section, in view of recent theoretical developments, and of the latest inputs on structure function fits. We show that the new CDF measurements are in good agreement with NLO QCD. If CDF preliminary data are confirmed, a long-standing discrepancy between NLO QCD predictions and hadron-collider data can be settled.

[*]Present address

arXiv:hep-ph/0312132v3 3 Jun 2004

Contents

1. Introduction

The measurement of the bottom quark production cross section in $p\bar{p}$ collisions has provided for the past fifteen years one of the most significant challenges to the ability of perturbative QCD to accurately predict absolute rates in hadronic collisions. Measurements of the transverse momentum (p_T) spectrum in the region $p_T > m_b$ (the bottom quark mass) have been performed by the UA1 experiment [1] at the $S\bar{p}pS$ ($\sqrt{S} = 630$ GeV) and by the CDF [2, 3, 4] and D0 [5] experiments at the Tevatron ($\sqrt{S} = 1.8$ TeV). Comparisons of Tevatron data with next-to-leading-order (NLO, i.e. $\mathcal{O}(\alpha_s^3)$) predictions [6, 7] have shown a systematic excess. The precise size of this excess depends on the input parameters used for the theoretical calculation, which is affected by an uncertainty of up to 50% due to the choice of renormalization and factorization scales (μ_R, μ_F) and by additional uncertainties due to the choice of parton distribution functions (PDFs) and of the value of the b quark mass. Nevertheless, the central value of the NLO prediction has typically been quoted as being smaller than the data by factors varying between 2 and 3.

Aside from the radical and interesting hypothesis that physics beyond the standard model is at work [8], the source of this discrepancy in the context of QCD has been searched for in various directions. At the perturbative level, the large scale dependence at NLO is a symptom of large higher-order contributions. First of all it is well known that there are new partonic processes which appear first at $\mathcal{O}(\alpha_s^3)$(such as gluon splitting). Furthermore, there are large logarithmic corrections which are present at all orders of perturbation theory. These can arise from several sources: on one side there are logarithms of the ratio of the hadronic center of mass energy and the quark mass [6, 9, 10] (the so-called small-x effects, $x \sim m_b/\sqrt{S}$). On the other, multiple gluon radiation leads at large p_T to towers of logarithms of p_T/m_b [11]. At the non-perturbative level, it has been noted [12] that the p_T spectrum of b hadrons (H_b) in hadronic collisions has a large sensitivity to the parameterization of the $b \to H_b$ fragmentation function, $D_b(z)$. Even assuming the applicability of the factorization theorem, an assumption which at low p_T remains to be validated, it is therefore crucial to ensure that the extraction of $D_b(z)$ from e^+e^- data is

performed in a fashion consistent with its application in the context of hadronic collisions, an issue often overlooked in the past.

The quantitative analysis of small-x effects in b production has followed several types of approaches. Some of them [13] do not attempt to include the exact NLO results, thus leading to a radical departure from the QCD-improved parton model. These approaches generally lead to very large K factors for heavy flavour production, even at high p_T, where these effects should be reduced. Large effects, strongly dependent on the chosen fit of unintegrated gluon densities, are also found in the small-x MC implementation of Jung [14]. The approach of Collins and Ellis [9] aims instead at computing the small-x enhanced effects that are *not already included* in the NLO results. In this approach one finds at the Tevatron corrections not larger than 20-30%.

The resummation of the logarithms of p_T/m_b, with next-to-leading logarithmic accuracy (NLL), and the matching with the fixed-order, exact NLO calculation for massive quarks, has been performed in [15] (FONLL).[1] A calculation with this level of accuracy is also available for b production in e^+e^- collisions [17], and has been used for the extraction of non-perturbative fragmentation functions from LEP and SLC data [18]. The equivalence of the perturbative inputs allows one to consistently convolute these functions with the FONLL b-quark spectra in hadronic collisions, leading to FONLL predictions for the H_b spectrum. A comparison of these predictions with CDF data at 1.8 TeV for $B^\pm$-meson production in the range 6 GeV $< p_T <$ 20 GeV has been presented in [19]. There the ratio between data and theory, averaged over the given p_T range, was reduced to a factor of 1.7, compatible with the residual theoretical and experimental uncertainties. This finding is consistent with experimental evidence from D0 (see the last paper in [5]) that the inclusive rate of jets containing b quarks – a quantity largely insensitive to the details of the perturbative and non-perturbative fragmentation – agrees with NLO QCD [20].

Non-perturbative fragmentation effects are expected to play a much reduced role in the prediction of the total production rate, as they only smear the p_T spectrum of the quark. Furthermore, effects due to initial-state multiple-gluon emission average to 0 after p_T integration. It follows that the measurement of b production down to $p_T \sim 0$ provides a crucial input for clarifying the origin of the residual discrepancy between QCD and data: an improved agreement would strongly support the idea that the blame rests on our incomplete understanding of the fragmentation phase. A residual, or increased, disagreement, would support the relevance of small-x effects, which are expected to grow at low p_T. For this reason, the recent CDF release [21] of preliminary data on H_b production at $\sqrt{S} = 1.96$ TeV in the domain $p_T > 0$, $|y_{H_b}| < 0.6$ provides us with a new, crucial input. In this paper we therefore re-evaluate the theoretical predictions developed in [19], extending the range in p_T down to 0, and reviewing the theoretical systematics. In addition, we compare these results with those obtained using the MC@NLO code [22], which merges the full NLO matrix elements with the complete shower evolution and hadronization performed by the HERWIG Monte Carlo. As discussed in detail in [22], this comparison probes a few features

---

[1]The matching with the massive result at low p_T is essential, due to the large size of mass corrections up to $p_T \sim 20$ GeV. Lack of mass effects [16] will therefore erroneously overestimate the production rate at small p_T.

where FONLL and MC@NLO differ by effects beyond NLO: the evaluation of subleading logarithms in higher-order emissions, in particular in the case of gluon emission from the b quark, and the hadronization of the heavy quark, which in MC@NLO is performed through HERWIG's cluster model, tuned on $Z^0 \to H_b X$ decays.

2. Theoretical results and uncertainties

We start by considering the integrated cross section for b quarks, reported by CDF in the domain $p_T > 0$, $|y_b| < 1$. This depends only indirectly on the fragmentation and on the resummation of p_T logarithms, so we start by quoting the results obtained with the standard NLO calculation. The total cross section is defined by the integral of the single-inclusive p_T distribution, with renormalization and factorization scales defined by $\mu_{R,F} = \xi_{R,F} \mu_0$, where $\mu_0^2 = p_T{}^2 + m_b^2$. The central values of our predictions are obtained with $\xi_{R,F} = 1$ and $m_b = 4.75$ GeV. To avoid the accidental compensation between the μ_F and the μ_R dependence of the cross section occurring when the two scales are kept equal, we compute the scale uncertainty by varying μ_R and μ_F independently over the range $0.5 < \xi_{R,F} < 2$, with the constraint $0.5 < \xi_R/\xi_F < 2$. The mass uncertainty corresponds to the range 4.5 GeV $< m_b < 5$ GeV. The result, using CTEQ6M [23] as PDF, is:

$$\sigma_b^{\mathrm{NLO}}(|y_b| < 1) = 23.6 \begin{smallmatrix} +4.5 \\ -3.6 \end{smallmatrix}_{m_b} \begin{smallmatrix} +10.8 \\ -6.3 \end{smallmatrix}_{\mu_R,\mu_F} \mu\mathrm{b} \ . \tag{2.1}$$

For comparison, the full FONLL calculation and MC@NLO lead to slightly larger central values, 25.0 μb and 25.2 μb respectively. This difference is due to higher-order effects included in these calculations, which render the rapidity distribution narrower than that computed at the NLO.

We studied the PDF uncertainties using three different sets of fits with systematics: CTEQ6 [23], MRST [24] and Alekhin [25]. Following the prescriptions in those papers, we get:[2]

$$\sigma_b^{\mathrm{NLO}}(|y_b| < 1, \mathrm{CTEQ}) = 23.6 \pm 2.3_{\mathrm{PDF}} \ \mu\mathrm{b} \ , \tag{2.2}$$

$$\sigma_b^{\mathrm{NLO}}(|y_b| < 1, \mathrm{MRST}) = 20.8 \pm 0.9_{\mathrm{PDF}} \ \mu\mathrm{b} \ , \tag{2.3}$$

$$\sigma_b^{\mathrm{NLO}}(|y_b| < 1, \mathrm{Alekhin}, \mathrm{FFN}) = 24.3 \pm 1.3_{\mathrm{PDF}} \ \mu\mathrm{b} \ , \tag{2.4}$$

$$\sigma_b^{\mathrm{NLO}}(|y_b| < 1, \mathrm{Alekhin}, \mathrm{VFN}) = 22.4 \pm 1.2_{\mathrm{PDF}} \ \mu\mathrm{b} \ . \tag{2.5}$$

The two Alekhin values refer to the choice of the fixed (FFN) and variable (VFN) flavour number schemes. We note that the CTEQ prediction has an uncertainty twice as large as the others. This is a known fact, related to the different prescriptions used to define the error ranges. A similar result holds in fact for other observables [27]. Secondly, we note that the MRST central value is only barely consistent with the others, even within the error bars.
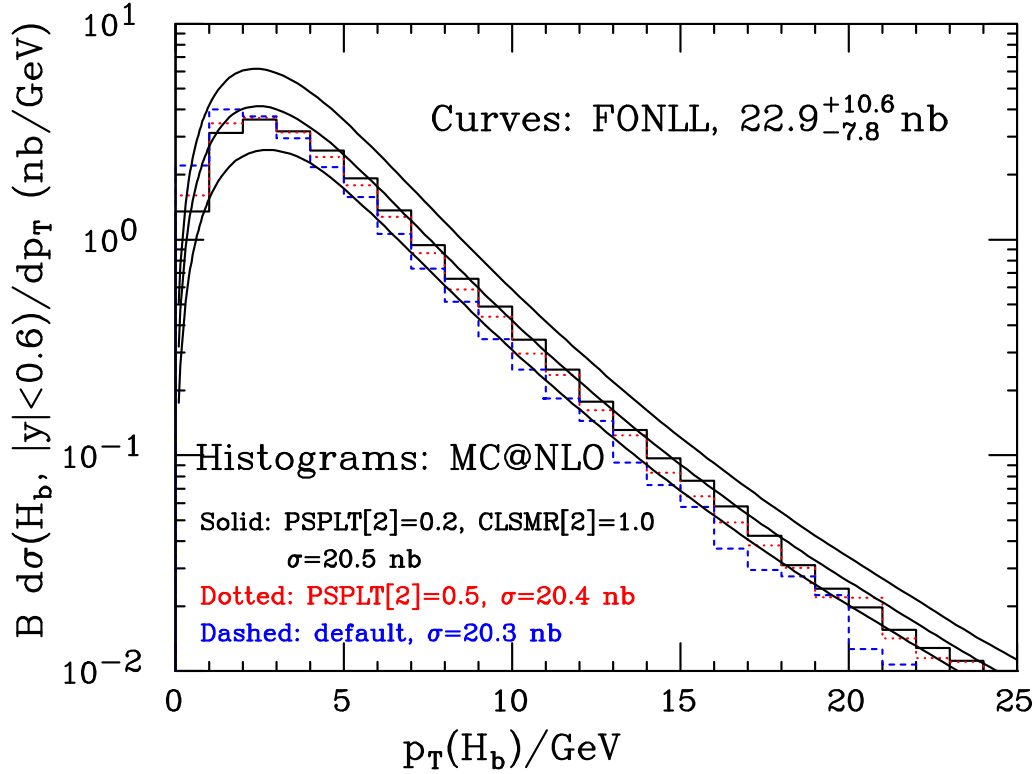
---

[2]We verified that the prescription proposed for CTEQ's sets in [26] leads to minimal differences in the results.

Figure 1: Lower panel: variations of the FONLL b-quark p_T spectrum ($y_b = 0$) due to PDF uncertainties, normalized to the central CTEQ prediction. Upper panel: variation of the spectrum due to scale and mass variations, normalized to the default prediction.

We move now to the FONLL analysis of the p_T spectra. The lower panel of Fig. 1 shows the PDF uncertainty of the b-quark p_T spectrum at $y_b = 0$. We plot the upper and lower results obtained using the CTEQ6, MRST and Alekhin fits, normalized to the central CTEQ6M prediction. In all cases, $m_b = 4.75$ GeV and $\xi_{R,F} = 1$. The spectrum confirms a poor consistency between MRST results and the others. Only for $p_T > 100$ GeV the three bands are consistent with each other. In the region below ~ 50 GeV, the theoretical uncertainty is however dominated by the effects of scale and mass variation, which are shown in the upper panel of Fig. 1. The scale variation is obtained by varying μ_R and μ_F as was done for the total rates. What we show is the envelope of the upper and lower results. The points on the curves therefore do not necessarily all correspond to the same scale choice, and the shape is not representative of a specific scale choice.

We summarize these results in Fig. 2, while at the same time going from the quark to the hadron level. The solid curves give the error band for the $p_T(H_b)$ spectrum as predicted by FONLL by summing in quadrature the scale, mass and PDF uncertainties. We selected CTEQ6M for our central prediction, and applied a 10% PDF uncertainty in each p_T bin, to reflect the effects shown in Fig. 1. The inclusion of non-perturbative effects related to the $b \rightarrow H_b$ fragmentation has been performed according to the framework described
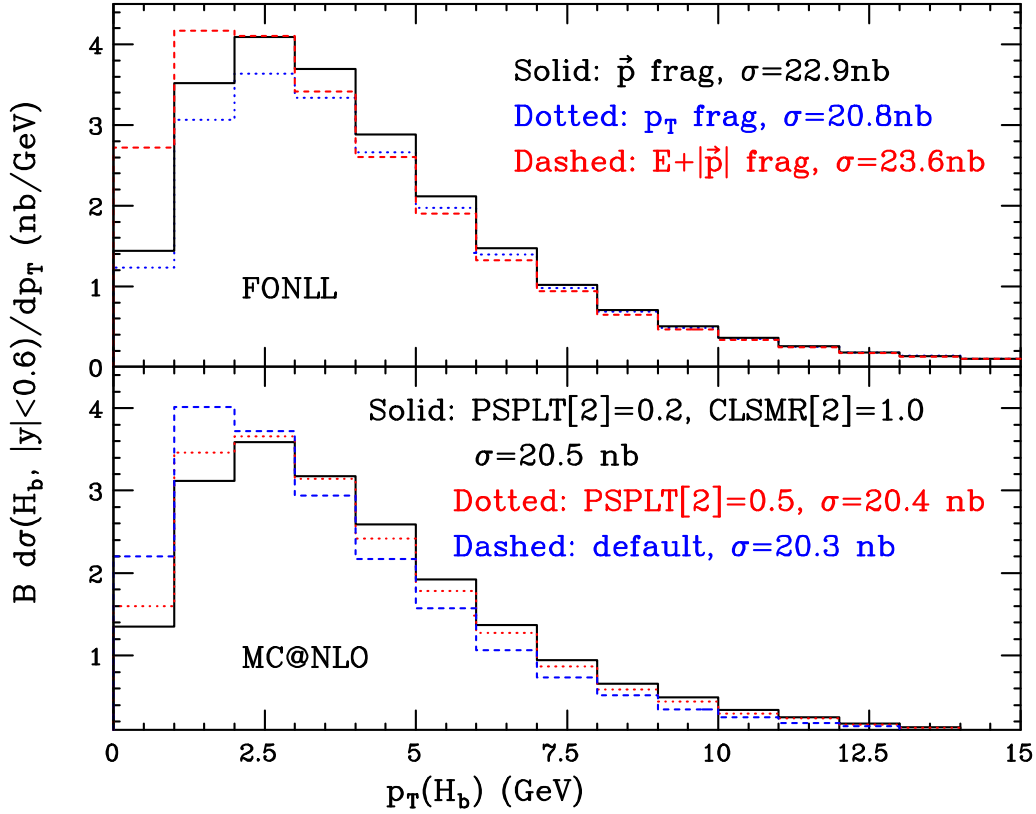
Figure 2: The H_b spectrum for $|y_{H_b}| < 0.6$. H_b stands for a b or $\bar{b}$ flavoured hadron. The cross section has been multiplied by $B \equiv BR(H_b \to J/\Psi \to \mu^+ \mu^-) = 6.82 \times 10^{-4}$ for future convenience. The solid curves give the FONLL overall uncertainty band as described in the text. The central solid curve corresponds to the central value, namely that obtained with CTEQ6M, $\mu = \mu_0$, and $m_b = 4.75$ GeV. The histograms present MC@NLO results obtained with different b hadronization parameters.

in [19]. The momentum fraction z (see below) used in this approach for scaling the b quark momentum to the H_b hadron one is extracted from a normalized Kartvelishvili et al. distribution, $D(z) = (\alpha + 1)(\alpha + 2)x^\alpha(1 - x)$ [28]. The phenomenological parameter α is fixed to 25.6, 29.1, 34 for $m_b = 4.5$, 4.75 and 5 GeV respectively by tuning it to moments of e^+e^- data (see [19]). We emphasize that these values for α depend also on other details and parameters of the perturbative calculation (like, for instance, the value of the strong coupling α_s), and cannot therefore simply be used with other b-quark perturbative spectra without retuning them to e^+e^- data.

In Fig. 2 we also present the results obtained with MC@NLO, using default values of mass, scales and PDF,[3] and for various choices of the b hadronization parameters, as described in [22]. The dashed histogram corresponds to the HERWIG default, whereas the solid (dotted) histogram has been obtained by setting PSPLT(2)=0.2 and CLSMR(2)=1 (PSPLT(2)=0.5). The agreement with the central FONLL prediction is satisfactory in terms

---

[3]We verified that mass, scale, and PDF uncertainties in MC@NLO are of the same size as those in FONLL.

Figure 3: Dependence of the $p_T(H_b)$ spectrum on the choice of fragmentation prescription in FONLL (upper panel), and on the b hadronization parameters in MC@NLO (lower panel, same curves as in Fig. 2).

of shape and rate in the case of the solid histogram; the other two choices of b hadronization parameters are seen to return softer $p_T(H_b)$ spectra.

Different choices of the b hadronization parameters in HERWIG correspond to different treatments of fragmentation in FONLL; the latter give additional uncertainties with respect to those, of purely perturbative origin, that we discussed so far. Here, we shall not study the fragmentation uncertainties systematically, and we shall limit ourselves to illustrate the typical sizes of these effects. As a result, we shall not cumulate the effect of the following variations with those above. The choice of the fragmentation variable for the $b \to H_b$ transition, which at high p_T is irrelevant, may lead to some differences at small p_T, where non-factorizable effects can be significant. The upper panel of Fig. 3 shows the effect of three separate choices of fragmentation. The solid line is the default used in this work, $\vec{p}(H_b) = z\vec{p}(b)$, the three-momenta being taken in the laboratory frame (the curves in Fig. 2 have been obtained with this choice). The dotted line corresponds to $p_T(H_b) = zp_T(b)$ and $y_{H_b} = y_b$. The dashed line to $(E + p)_{H_b} = z(E + p)_b$. For comparison, the lower panel of Fig. 3 presents the MC@NLO results already shown in Fig. 2. Different fragmentation/hadronization choices lead to different shifts in y_{H_b}, which can have an impact on the cross section within the $|y_{H_b}| < 0.6$ range when $p_T \lesssim m_b$.

For FONLL, these shifts modify the total rate at the level of $\sim 10\%$, while no significant change is observed with the MC@NLO hadronization. This is not surprising, since the fragmentation mechanism is strictly speaking only applicable in the large-p_T region, while the hadronization embedded into parton shower Monte Carlos should work for any p_T's (and thus requires more tuning to data).

3. Comparison with experimental data

We present now the comparison of our results with data. Since the CDF measurement is performed using inclusive $B \to J/\psi + X$ decays, with $J/\psi \to \mu^+\mu^-$, we first quote results for this observable. The FONLL prediction uses the $B \to J/\psi + X$ spectra measured by BaBar and CLEO [29], applied to all H_b states. We verified that the $p_T(J/\psi)$ distribution shows little sensitivity to the input choice for the decay spectrum. On the other hand, MC@NLO generates the $B \to J/\psi + X$ decays using the perturbative $b \to c$ decay spectrum. The resulting $p_T(J/\psi)$ spectra are compared in Fig. 4. At variance with the case of Fig. 2, the J/ψ spectra predicted by MC@NLO are generally harder than that predicted by FONLL. The best agreement is obtained with the choice of the b hadronization parameters that gives the worst agreement in the case of the $p_T(H_b)$ spectrum. Since the $B \to J/\psi$ fragmentation in FONLL is obtained directly from data, this points out that a more realistic treatment of the B decay would be needed in HERWIG. Clearly, this effect can be eliminated by replacing the internal HERWIG B-decay routines with standard B-decay packages.

Defining $\sigma_{J/\psi} = \sigma(H_b \to J/\psi, p_T(J/\psi) > 1.25, |y_{J/\psi}| < 0.6) \times \mathrm{BR}(J/\psi \to \mu^+\mu^-)$, where [30]

$$\mathrm{BR}(J/\psi \to \mu^+\mu^-) = 5.88 \times 10^{-2}$$

and, to be used below,

$$\mathrm{BR}(H_b \to J/\psi) = 1.16 \times 10^{-2} \ ,$$

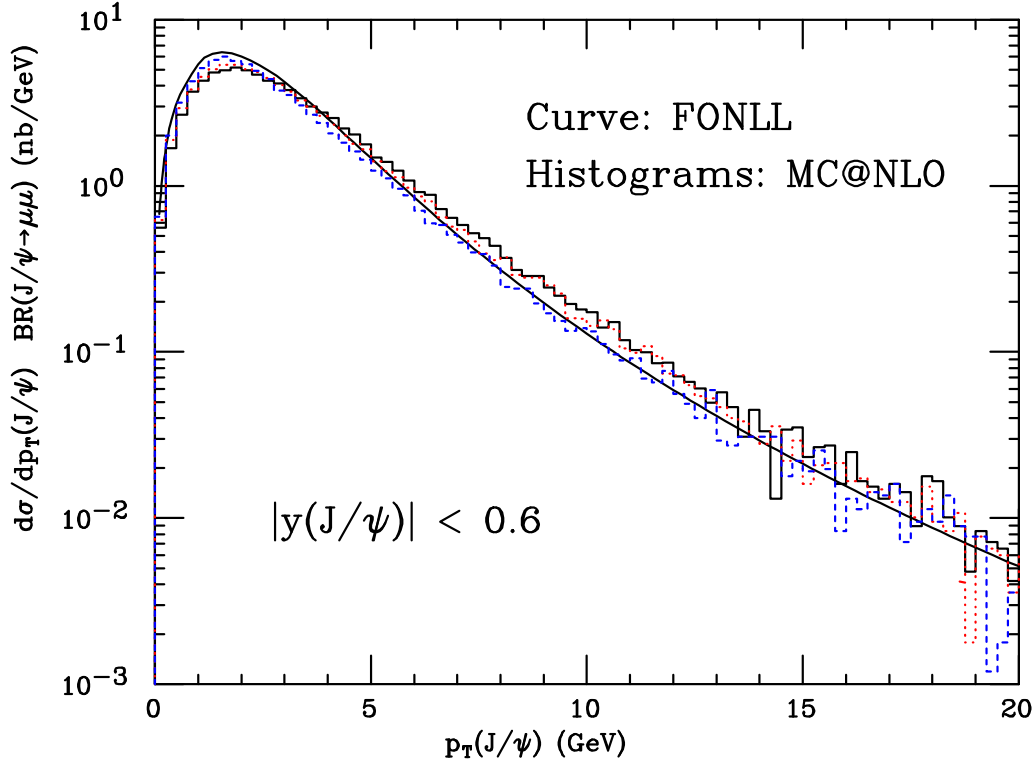$$B \equiv \mathrm{BR}(H_b \to J/\psi \to \mu^+\mu^-) = 6.82 \times 10^{-4} \ ,$$

CDF's result is:

$$\sigma_{J/\psi}^{\mathrm{CDF}} = 19.9 \ {}^{+3.8}_{-3.2 \, stat+syst} \ \mathrm{nb} \ , \tag{3.1}$$

in excellent agreement with ours:

$$\sigma_{J/\psi}^{\mathrm{FONLL}} = 18.3 \ {}^{+8.1}_{-5.7} \ \mathrm{nb} \ , \tag{3.2}$$

where we combined in quadrature the uncertainties from scale, mass and PDF variations. CDF then deconvolutes the $H_b \to J/\psi$ decay, quoting the following result for $\sigma_{H_b} = \sigma(H_b, |y_{H_b}| < 0.6) \times B$:

$$\sigma_{H_b}^{\mathrm{CDF}} = 24.5 \ {}^{+4.7}_{-3.9 \, stat+syst} \ \mathrm{nb} \ , \tag{3.3}$$

Figure 4: FONLL prediction for the J/ψ spectrum (solid curve), for central values of mass, scales, PDF, and fragmentation scheme, compared to MC@NLO results (histograms).

in good agreement with our estimate:

$$\sigma_{H_b}^{\text{FONLL}} = 22.9 \ ^{+10.6}_{-7.8} \, \text{nb} \ . \tag{3.4}$$

After dividing the H_b rate by a factor $B \times 0.61$ to correct for the branching ratio and for the different y_b range,[4] CDF gives a b-quark cross section for $|y_b| < 1$:

$$\sigma_b^{\text{CDF}}(|y_b| < 1) = 29.4 \ ^{+6.2}_{-5.4} {}_{\, stat+syst} \, \mu\text{b} \ , \tag{3.5}$$
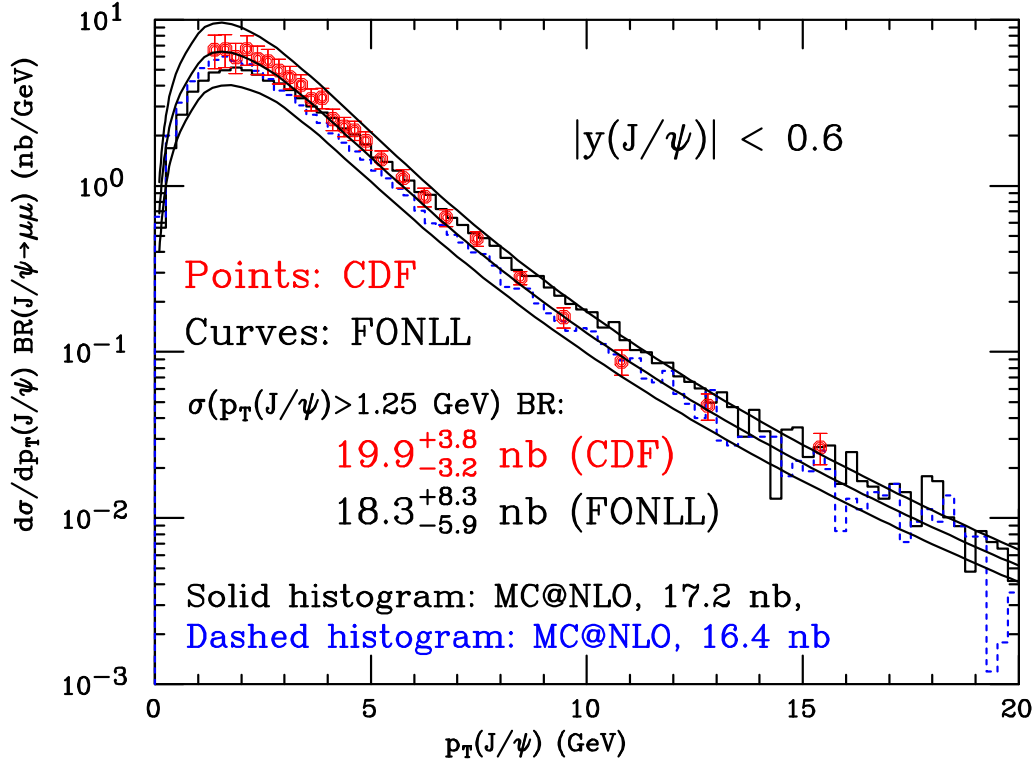
to be compared with our estimate (Eq. (2.1) with the additional 10% PDF uncertainty, rescaled to the FONLL result):

$$\sigma_b^{\text{FONLL}}(|y_b| < 1) = 25.0 \ ^{+12.6}_{-8.1} \, \mu\text{b} \ . \tag{3.6}$$

We note that the difference between the central values of data and theory increases from 5% to 15% when going from the result closest to the direct experimental measurement (the J/ψ cross section) to those which require more deconvolution and acceptance corrections (the inclusive b quark rate). This seems to indicate intrinsic differences, to be ultimately considered as part of the systematic error, in the modeling of the transition from the quark

---

[4]The correction factor for the y_b range predicted by FONLL and MC@NLO is also 0.61.
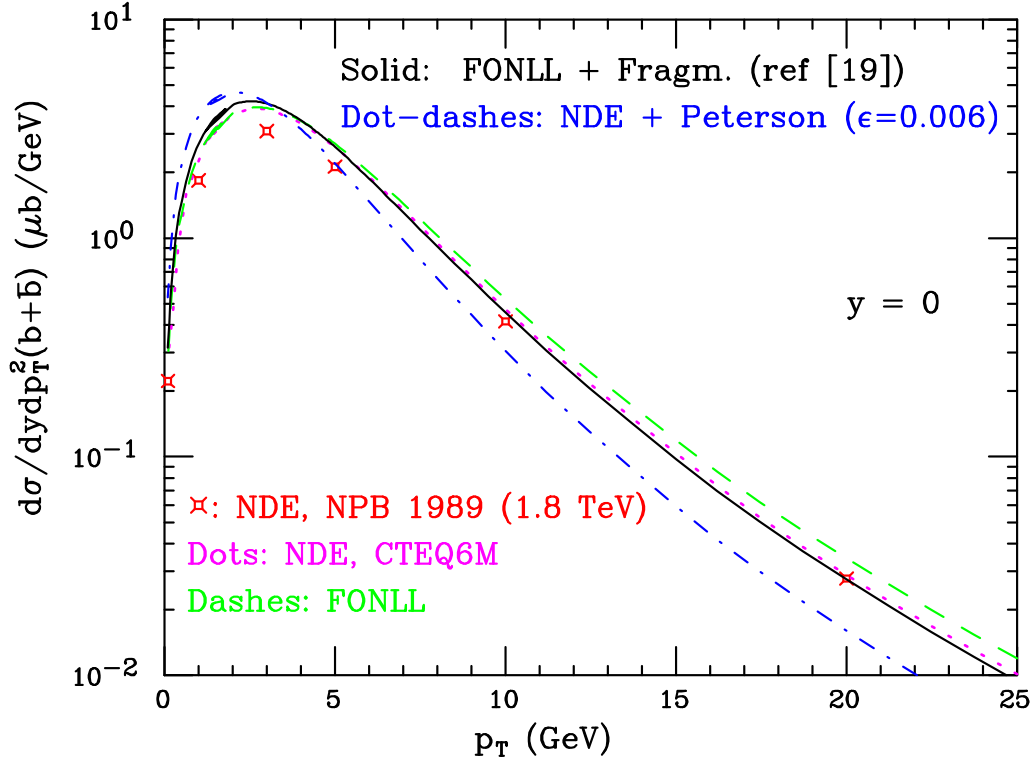
Figure 5: CDF J/ψ spectrum from B decays. The theory band represents the FONLL systematic uncertainties, propagated from Fig. 2. Two MC@NLO predictions are also shown (histograms), with the same patterns as in Fig. 3.

to the hadrons, and vice versa. Effects of this size are consistent with what we showed in Fig. 3.

We finally present in Fig. 5 our prediction for the J/ψ spectrum, obtained by convoluting the FONLL result with the J/ψ momentum distribution in inclusive $B \to J/\psi + X$ decays.[5] The data lie well within the uncertainty band, and are in very good agreement with the central FONLL prediction. We also show the two MC@NLO predictions corresponding to the two extreme choices of the b hadronization parameters considered in this work; very good agreement with data is obtained for one of them in terms of shape, with the normalization being slightly low (still within 1σ of the mass and scale uncertainties).

We stress that both FONLL and MC@NLO are based on the NLO result of [7] (henceforth referred to as NDE), and only marginally enhance the cross section predicted there, via some higher-order effects. The most relevant change in FONLL with respect to old predictions lies at the non-perturbative level, i.e. in the treatment of the $b \to H_b$ hadronization, which makes use [19] of the moment-space analysis of the most up-to-date data on b fragmentation in e^+e^- annihilation. The evolution of the NLO theoretical predictions over time
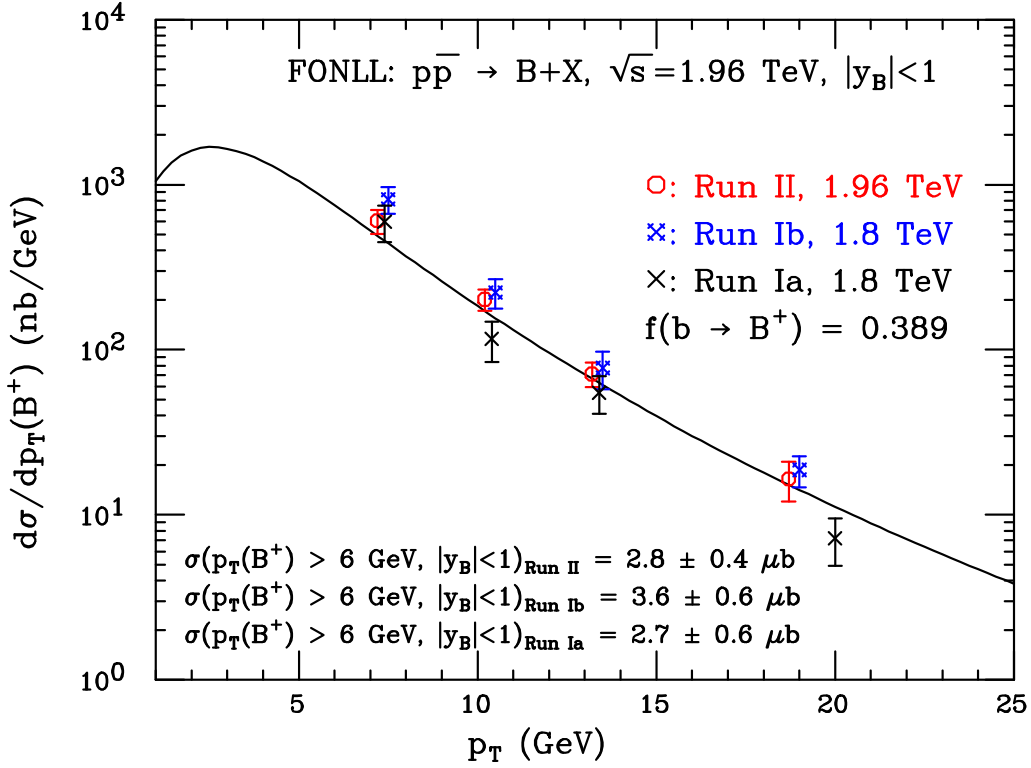
---

[5]An earlier version of this work had a curve with a slightly different slope. We correct here an accidental error in the treatment of the H_b decay: in the previous version the b-quark mass, instead of the b-hadron mass (which we take equal to 5.3 GeV), was used in the boost to the H_b rest frame before its decay.

Figure 6: Evolution of the NLO QCD predictions over time, for $\sqrt{S} = 1800$ GeV.

is shown in Fig. 6. Here we plot the original central prediction of NDE for $\sqrt{S} =$1.8 TeV (symbols), obtained using NLO QCD partonic cross sections convoluted with the PDF set available at the time, namely DFLM260 [31]. The same calculation, performed with the CTEQ6M PDF set (dotted curve), shows an increase of roughly 20% in rate in the region $p_T < 10$ GeV. The effect of the inclusion of the resummation of NLL logarithms is displayed by the dashed curve, and is seen to be modest in the range of interest. Finally, we compare the original NDE prediction after convolution with the Peterson fragmentation function ($\epsilon = 0.006$, dot-dashed curve), with the FONLL curve convoluted with the fragmentation function extracted in [19] (solid curve). Notice that the effect of the fragmentation obtained in [19] brings about a modest decrease of the cross section (the difference between the dashed and solid curves), while the traditional Peterson fragmentation with $\epsilon = 0.006$ has a rather pronounced effect (the difference between the symbols and the dot-dashed curve). Thus, the dominant change in the theoretical prediction for heavy flavour production from the original NDE calculation up to now appears to be the consequence of more precise experimental inputs to the bottom fragmentation function [18], that have shown that non-perturbative fragmentation effects in bottom production are much smaller than previously thought.

We recall once more that, at the level of central values and neglecting the theoretical and experimental uncertaintites, the FONLL result [19], using CTEQ5M PDF, underestimates CDF's run IB $B^{\pm}$ rate [4] for $p_T \gtrsim 6$ GeV by a factor of 1.7. The main improve-

Figure 7: Evolution of the CDF data for exclusive $B^\pm$ production: Run IA[3], Run IB [4] and Run II[21].

ment in the comparison between Run II data and theory comes from the new CDF data, which tend to be lower than one would have extrapolated from the latest measurements at 1.8 TeV. To clarify this point, we collect in Fig. 7 the experimental results from the CDF measurements of the $B^\pm$ cross section in Run IA [3], in Run IB [4] and in Run II. The rate in the bin which in the past showed the worse discrepancy, namely the first bin corresponding to $p_T(B^\pm) > 6$ GeV, evolved from 2.7 ± 0.6 μb (Run IA) to 3.6 ± 0.6 μb (Run IB), and decreased to 2.8 ± 0.4 μb in Run II. The increase in the c.m. energy should have instead led to an increase by 10-15%. The Run II result is therefore lower than the extrapolation from Run IB by approximately 30%. By itself, this result alone would reduce the factor of 1.7 quoted in [19] to 1.2 at $\sqrt{S} = 1.96$ TeV. In addition, the results presented in this paper lead to an increase in rate relative to the calculation of [19] by approximately 10-15%, due to the change of PDF from CTEQ5M to CTEQ6M. The combination of these two effects, dominated in any case by the lower normalization of the new data, leads to the excellent agreement observed in our work. We then conclude that the improved agreement between the Run II measurements and perturbative QCD is mostly a consequence of improved experimental inputs (which include up-to-date α_s and PDF determinations).

4. Conclusions

In summary, the recent CDF measurement of total b-hadron production rates in $p\bar{p}$ collisions at $\sqrt{S} = 1.96$ TeV is in good agreement with NLO QCD, the residual discrepancies being well within the uncertainties due to the choice of scales and, to a lesser extent, of mass and PDF. A similar conclusion is reached for the p_T spectrum, where the calculation is improved by the inclusion of the NLL resummation of collinear logarithms. The improvement in the quality of the agreement between data and theory relative to previous studies is the result of several small effects, ranging from a better knowledge of fragmentation and structure functions and of α_s, which constantly increased in the DIS fits over the years, to the fact that these data appear to lead to cross sections slightly lower than one would have extrapolated from the measurements at 1.8 TeV. The current large uncertainties in data and theory leave room for new physics. However there is no evidence now that their presence is required for the description of the data, and furthermore the recent results of [32] rule out the existence of a scalar bottom quark in the range preferred by the mechanism proposed in [8]. The data disfavour the presence of small-x effects of the size obtained with the approaches of refs. [13]. They are instead compatible with the estimates of [9]. We thus conclude that approaches to the small-x problem that can exactly include the NLO corrections (i.e. that can be used to perform a consistently matched calculation) should be further pursued, also in light of the recent progress in small-x resummation [33]. It is not unlikely that the consistent inclusion of small-x effects could further reduce the theoretical errors due to scale variation and PDF uncertainties. A final confirmation of the CDF data, as well as the extension of the measurements to the high-p_T region ($p_T > 40$ GeV), where the theoretical uncertainty from scale variations is significantly reduced, would provide additional support to our conclusions. While our work has no direct impact on other anomalies reported by CDF in the internal structure and correlations of heavy-flavoured jets [34], we do expect that the improvements relative to pure parton-level calculations present in the MC@NLO should provide a firmer benchmark for future studies of the global final-state stucture of $b\bar{b}$ events.

References

[1] C. Albajar *et al.*, [UA1], Phys. Lett. **B186**, 237 (1987); Phys. Lett. **B256**, 121 (1991).

[2] F. Abe *et al.*, [CDF], Phys. Rev. Lett. **71**, 500 (1993); Phys. Rev. Lett. **71**, 2396 (1993); Phys. Rev. D**50** (1994) 4252; D. Acosta *et al.*, [CDF], Phys. Rev. D**66** (2002) 032002.

[3] F. Abe *et al.* [CDF Collaboration], Phys. Rev. Lett. **75** (1995) 1451.

[4] D. Acosta *et al.* [CDF Collaboration], Phys. Rev. D **65** (2002) 052005.

[5] S. Abachi *et al.*, [D0], Phys. Rev. Lett. **74** (1995) 3548; B. Abbott *et al.*, [D0], Phys. Rev. Lett. **84** (2000) 5478; Phys. Lett. **B487**, 264 (2000); Phys. Rev. Lett. **85** (2000) 5068.

[6] P. Nason, S. Dawson, and R. K. Ellis, Nucl. Phys. **B303** (1988) 607.

[7] P. Nason, S. Dawson, and R. K. Ellis, Nucl. Phys. **B327** (1989) 49, and erratum-ibid. B**335** (1989) 260.; W. Beenakker *et al.*, Nucl. Phys. **B351** (1991) 507.

[8] E. L. Berger *et al.*, Phys. Rev. Lett. **86** (2001) 4231.

[9] J. C. Collins and R. K. Ellis, Nucl. Phys. B**360** (1991) 3. See also R. D. Ball and R. K. Ellis, JHEP **0105** (2001) 053.

[10] S. Catani, M. Ciafaloni and F. Hautmann, Nucl. Phys. B**366** (1991) 135.

[11] M. Cacciari and M. Greco, Nucl. Phys. B**421** (1994) 530.

[12] M. L. Mangano, hep-ph/9711337; S. Frixione, M. L. Mangano, P. Nason, and G. Ridolfi, "Heavy Flavors II", eds. A.J. Buras and M. Lindner, Adv. Ser. Direct. High Energy Phys. **15** (1998) 609.

[13] E. M. Levin, M. G. Ryskin, Y. M. Shabelski and A. G. Shuvaev, Sov. J. Nucl. Phys. **53** (1991) 657. S. P. Baranov and M. Smizanska, Phys. Rev. D**62** (2000) 014012. S. P. Baranov, A. V. Lipatov and N. P. Zotov, hep-ph/0302171.

[14] H. Jung, Phys. Rev. D**65** (2002) 034015; Mod. Phys. Lett. A **19** (2004) 1.

[15] M. Cacciari, M. Greco and P. Nason, JHEP **9805**, 007 (1998).

[16] J. Binnewies, B. A. Kniehl and G. Kramer, Phys. Rev. D**58** (1998) 034016.

[17] P. Nason and C. Oleari, Nucl. Phys. B **565** (2000) 245. B. Mele and P. Nason, Nucl. Phys. **B361**, 626 (1991); G. Colangelo and P. Nason, Phys. Lett. **B285**, 167 (1992).

[18] A. Heister *et al.*, [Aleph], Phys. Lett. **B512**, 30 (2001); K. Abe *et al.* [SLD], Phys. Rev. D**65** (2002) 092006 [Erratum-ibid. D**66** (2002) 079905].

[19] M. Cacciari and P. Nason, Phys. Rev. Lett. **89** (2002) 122003.

[20] S. Frixione and M. L. Mangano, Nucl. Phys. B **483** (1997) 321.

[21] C. Chen, [CDF], presentation at "Beauty 2003", http://www-cdf.fnal.gov/physics/new/bottom/030904.blessed-bxsec-jpsi/ ; M. Bishai [CDF], presentation at Fermilab, Dec 5. 2003, http://www-cdf.fnal.gov/~bishai/papers/wandc.pdf

[22] S. Frixione, P. Nason and B. R. Webber, JHEP **0308** (2003) 007; S. Frixione and B. R. Webber, JHEP **0206** (2002) 029.

[23] J. Pumplin et al., JHEP **0207** (2002) 012.

[24] A. D. Martin, R. G. Roberts, W. J. Stirling and R. S. Thorne, Eur. Phys. J. C **28** (2003) 455.

[25] S. Alekhin, Phys. Rev. D**68** (2003) 014002.

[26] Z. Sullivan, Phys. Rev. D**66** (2002) 075011.

[27] D. Stump et al., JHEP **0310** (2003) 046; M. Cacciari, S. Frixione, M. L. Mangano, P. Nason and G. Ridolfi, JHEP **0404** (2004) 068; A. Djouadi and S. Ferrag, Phys. Lett. B **586** (2004) 345.

[28] V. G. Kartvelishvili, A. K. Likhoded and V. A. Petrov, Phys. Lett. B **78** (1978) 615.

[29] B. Aubert *et al.* [BABAR], Phys. Rev. D**67**, 032002 (2003). S. Anderson *et al.* [CLEO], arXiv:hep-ex/0207059.

[30] K. Hagiwara *et al.* [Particle Data Group Collaboration], Phys. Rev. D **66** (2002) 010001.

[31] M. Diemoz, F. Ferroni, E. Longo and G. Martinelli, Z. Phys. C **39** (1988) 21.

[32] P. Janot, arXiv:hep-ph/0403157.

[33] M. Ciafaloni, D. Colferai, G. P. Salam and A. M. Stasto, Phys. Rev. D **68** (2003) 114003;
G. Altarelli, R. D. Ball and S. Forte, arXiv:hep-ph/0310016.

[34] D. Acosta *et al.* [CDF Collaboration], Phys. Rev. D **65** (2002) 052007;
Phys. Rev. D **69** (2004) 012002; Phys. Rev. D **69** (2004) 072004.